

# A Generalized Solution to the Spectral Efficiency Loss in Unipolar Optical OFDM-based Systems

Mohamed Sufyan Islim, Dobroslav Tsonev and Harald Haas

Li-Fi R&D Centre, Institute for Digital Communications, University of Edinburgh  
King's Buildings, Mayfield Road, Edinburgh, EH9 3JL, UK  
Email: {m.islim, d.tsonev, h.haas}@ed.ac.uk

**Abstract**—A number of unipolar optical orthogonal-frequency-division-multiplexing (OFDM) schemes have been proposed as a solution to the high energy consumption in the widely adopted direct-current-biased optical OFDM (DCO-OFDM) modulation scheme. These schemes have a reduced spectral efficiency due to the restrictions imposed on their frame structure. The enhanced unipolar OFDM (eU-OFDM) modulation scheme was recently introduced to compensate for the reduced spectral efficiency in unipolar OFDM (U-OFDM). The concept exploits the frame structure of U-OFDM and allows for multiple U-OFDM information streams to be combined, thus increasing the overall spectral efficiency of the communication system. In this paper, the concept of the enhanced U-OFDM scheme is generalized for arbitrary combinations of U-OFDM data streams with various constellation sizes and various power allocations. A closed-form theoretical bound on the bit error rate (BER) performance of the Generalized Enhanced Unipolar OFDM (GREENER-OFDM) is derived and verified by comparison with the results of Monte Carlo simulations. The proposed scheme has an improved power efficiency compared with a spectrally equivalent DCO-OFDM. The GREENER-OFDM allows the gap in spectral efficiency between DCO-OFDM and the inherently unipolar optical OFDM schemes to be completely closed.

## I. INTRODUCTION

There is an increasing demand for system capacity in mobile services, and it is estimated that by 2018, data demand will be more than 15 Exabytes per month [1]. Current use of the electromagnetic spectrum is in the radio frequency (RF) ranges while other parts of the spectrum remain unused. The visible light spectrum, for example, offers hundreds of THz more bandwidth than radio frequency. Exploiting this spectrum range could satisfy the exponentially growing demand for data communication. A 3 Gbps visible light communication (VLC) link was recently reported [2] using a Gallium Nitride micro-light-emitting-diode ( $\mu$ LED). This result illustrates the large potential of VLC technology. In addition to its ability to deliver high-speed data transfer, VLC offers further benefits: it can be employed in restricted areas where sensitive electronic equipments are present; it provides an inherent security feature at the physical layer; the existing lighting infrastructure can be used to realize network access points (AP), which facilitates the integration of VLC into future heterogeneous networks. VLC has already been identified as a good candidate for many potential applications including but not limited to optical cellular networks, fixed high-speed bidirectional communication, vehicular communications, and underwater communications.

The physical properties of the conventionally employed front-end devices restrict the digital modulation schemes in VLC to intensity modulation and direct detection (IM/DD) techniques. Wireless optical signals are intensity modulated using light emitting diodes (LEDs) and are directly detected by photodiodes (PDs). Modulation schemes such as on-off keying (OOK), pulse width modulation (PWM), pulse position modulation (PPM), and pulse amplitude modulation (PAM) can be easily deployed in optical wireless communication systems [3]. However, in high data rate applications, these schemes experience inter-symbol interference (ISI) caused by the dispersive wireless optical channels and by the limited modulation bandwidth of the front-end elements [4]. That is why orthogonal frequency division multiplexing (OFDM) is often considered a more suitable modulation technique for optical wireless communication. A major advantage of OFDM is the capability of using adaptive modulation and low-complexity equalization. Radio frequency OFDM signals are both complex and bipolar. Therefore, a modification is required before OFDM becomes suitable for IM/DD systems. For example, Hermitian symmetry has to be imposed in the frequency domain during the OFDM signal generation process in order to obtain a real time-domain signal. Then, a modification of the time-domain signal is required in order to make it unipolar. A number of schemes that enable the use of OFDM in optical communication already exist, including: direct current optical OFDM (DCO-OFDM) [5]; asymmetrically clipped optical OFDM (ACO-OFDM) [6]; pulse amplitude modulated discrete multitone (PAM-DMT) [7]; flipped OFDM [8]; and unipolar OFDM (U-OFDM) [9]. The concept of DCO-OFDM is straightforward and has been proven in practice [2]. Its disadvantage, however, is the substantial energy dissipation due to the biasing requirements of the LED. The aim of introducing the other four schemes is to remove the biasing requirement and to improve the energy efficiency. All of the schemes, however, have a reduced spectral efficiency compared with DCO-OFDM [4] due to restrictions imposed on their frame structures. In [10], enhanced U-OFDM (eU-OFDM) is proposed to compensate for the spectral efficiency loss by superimposing multiple U-OFDM streams. However, only one variant of eU-OFDM, where all superimposed information streams employ the same constellation size, has so far been presented. In eU-OFDM, the spectral efficiency gap between U-OFDM and DCO-OFDM

can never be closed completely because this would require a large number of information streams (an infinite number in theory) to be superimposed in the modulation signal. In the current study, the enhanced U-OFDM concept is generalized to configurations where information streams with arbitrary constellation sizes and arbitrary power allocations can be employed. As a result, the spectral efficiency gap between U-OFDM and DCO-OFDM can be closed completely with an appropriate selection of the employed constellations in the different information streams superimposed in the modulation signal. The proposed scheme is compared with DCO-OFDM in the context of a linear flat additive white Gaussian noise (AWGN) channel.

The rest of this paper is organized as follows. In Section II, the DCO-OFDM and U-OFDM schemes are discussed. In Section III, the eU-OFDM and the GeneRalizEd EnhaNcEd unipolaR OFDM (GREENER-OFDM) are introduced. In Section IV, the theoretical bound on the BER performance of GREENER-OFDM is derived and validated by Monte Carlo simulations. In Section V, the optimal power allocations and constellation sizes configurations in GREENER-OFDM are compared with the DCO-OFDM scheme at different spectral efficiencies. Finally, Section VI gives the conclusions.

## II. UNIPOLAR OFDM SCHEME

DCO-OFDM is a low-complexity adaptation of the radio frequency OFDM to the optical domain [5]. Imposing Hermitian symmetry in the frequency domain restricts the OFDM output to be real and bipolar. Then a DC bias is introduced to the output waveform in order to convert it into a unipolar signal. However, time-domain OFDM signals typically attain a high peak to average power ratio (PAPR) which makes it practically impossible for the bias to turn all possible signal values to unipolar ones. Therefore, lower clipping of the DCO-OFDM signals is unavoidable. Following [11], the DC bias can be defined as a  $k$  multiple of the standard deviation of the time-domain OFDM signal  $\sigma_s$ . Then, the additional dissipation of electrical power in DCO-OFDM compared with bipolar OFDM can be written as [11]:

$$B_{DC}^{dB} = 10 \log_{10}(k^2 + 1). \quad (1)$$

The incurred penalty due to the bias increases as the modulation order,  $M$ , increases, which leads to electrical and optical power inefficiency when DCO-OFDM is used with high  $M$ -QAM modulation orders. This can be justified when the optical power in a visible light communication scenario is used for the purposes of both lighting and communication. However, when energy efficiency is required, an alternative modulation approach is required.

The high energy consumption of DCO-OFDM motivated the U-OFDM scheme being proposed in [9]. The principle of U-OFDM is to map each real bipolar OFDM frame into two unipolar frames. The first frame conveys the positive samples of the original bipolar frame with zeros at the positions of the negative samples; the second frame conveys the absolute values of the negative samples with zeros at the positions of the positive samples. As a result, U-OFDM creates a positive time

domain OFDM signal without the need of a DC-bias. However, the need for two frames to convey the information of a single DCO-OFDM frame decreases the spectral efficiency by half compared with DCO-OFDM. At the receiver, the original bipolar frame is obtained by subtracting the frame holding the negative values from the frame that holds the positive values. After this, conventional OFDM demodulation is applied on the reconstructed bipolar frame. This approach, however, doubles the noise at the receiver which results in a 3 dB SNR penalty compared with conventional bipolar OFDM.

## III. GREENER-OFDM

### A. Modulation Concept

For the same spectral efficiency, U-OFDM employs  $M^2$ -QAM when DCO-OFDM employs  $M$ -QAM. Since larger  $M$ -QAM constellations require more power, the power efficiency improvement of U-OFDM over DCO-OFDM decreases and quickly disappears as the constellation size  $M$  increases. This applies to all other similar unipolar schemes (ACO-OFDM, PAM-DMT, Flip-OFDM). This effect has led to the development of eU-OFDM [10] which aims to overcome the spectral efficiency loss of the unipolar OFDM schemes. The concept of eU-OFDM is to superimpose multiple U-OFDM time domain streams in order to form a single time domain eU-OFDM stream. A possible arrangement of the multiple U-OFDM signals is given in Fig. 1. The eU-OFDM frames are generated as follows. At depth-1, a U-OFDM time domain signal is generated as described in Section II. At depth-2, a second stream of U-OFDM is superimposed on the stream at depth-1. At depth-2, each unipolar frame is replicated twice. Since two U-OFDM frames contain the same information at depth-2, the amplitude of each frame is scaled by  $1/\sqrt{2}$  in order to preserve the overall signal energy at this depth. At depth-3, a third stream of U-OFDM is generated and superimposed in a similar way to the stream at depth-2. However, at depth-3, each unipolar U-OFDM frame is replicated four times and scaled by  $1/2$ . Additional U-OFDM streams can be added after they are replicated  $2^{d-1}$  times and scaled by  $1/\sqrt{2^{d-1}}$ , where  $d$  is the depth of the respective information stream. In addition to that, each of the streams is scaled by a parameter  $1/\gamma_d$  to facilitate the optimization of the allocated power to that stream. The scaling factor  $\gamma_d$  given in dB can be written as:

$$\gamma_d^{dB} = 20 \log_{10}(\gamma_d). \quad (2)$$

At the receiver, the demodulation process starts with demodulation of the data at depth-1 where a conventional U-OFDM receiver is used, as described in Section II. The inter-stream interference caused by the superposition of multiple U-OFDM streams is removed by the subtraction operation in the demodulation process since the interference on each positive frame at depth-1 is equivalent to the interference on each negative frame due to the stream structure imposed in the modulation process. After the information at depth-1 is demodulated, the recovered bits are remodulated at the receiver in order to reconstruct the information signal at depth-1, which is then subtracted from the overall received eU-OFDM signal. As a result, the

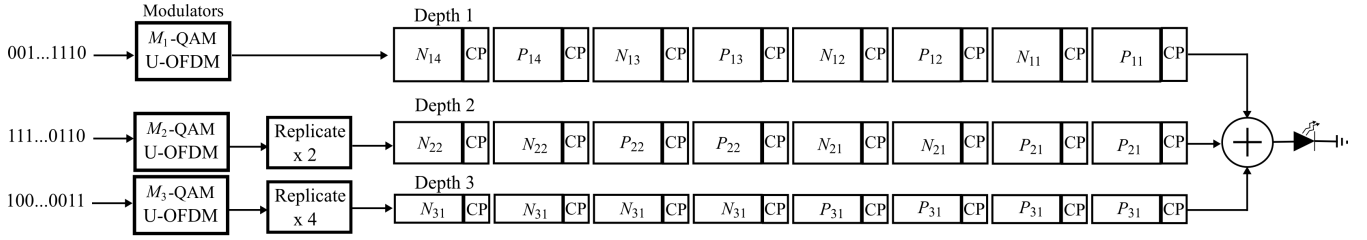


Fig. 1. Illustration of the enhanced U-OFDM concept with three information streams. CP represents the cyclic prefix,  $P_{kl}$  represents the positive U-OFDM frame, and  $N_{kl}$  represents the negative frame of U-OFDM. The subscripts denote that the frame at depth- $k$  belongs to the  $l$ -th original bipolar OFDM frame.

signal at depth-1 is completely removed from the received eU-OFDM signal. Afterwards, each two identical frames at depth-2 are summed. The demodulation process at depth-2 continues with the conventional U-OFDM demodulation algorithm and the recovered bits are remodulated in order to allow for the information stream at depth-2 to be subtracted from the overall received information signal. The demodulation process continues in a similar way for all subsequent streams until the information at all depths is recovered.

The spectral efficiency of eU-OFDM can be written as the sum of the spectral efficiencies of the information signals at all depths. This is expressed as [10]:

$$\eta_{eU}(D) = \sum_{d=1}^D \frac{\eta_U}{2^{d-1}} = \eta_U \sum_{d=1}^D \frac{1}{2^{d-1}} \quad (3)$$

where  $D$  is the number of depths used. Therefore, as  $D$  increases, the spectral efficiency of eU-OFDM approaches the spectral efficiency of DCO-OFDM. However, implementation issues put a practical limit on the maximum number of depths that can be used, including: latency, computational complexity and memory requirements. Moreover, each additional stream is added on top of an existing time domain signal formed by the streams at lower depths. Therefore, the energy per bit for each additional stream increases as the modulation depth increases. Considering that the spectral efficiency of each additional stream decreases exponentially, it can be assumed that practical implementation of eU-OFDM is likely to be realized using only a few information streams. The eU-OFDM was introduced as a special case of the GREENER-OFDM where it was assumed that the constellation size and the power allocation is the same for all information streams. However, in order for the spectral efficiency gap between eU-OFDM and DCO-OFDM to be completely closed, an alternative setting of constellation sizes at the modulation depths should be exploited. All possible combinations of constellation sizes at the different eU-OFDM streams with all possible power allocations are investigated in this study for a maximum depth of  $D = 3$ , where spectral efficiency in the range from 0.5 to 5 bits/s/Hz is achieved.

### B. Spectral Efficiency

As in eU-OFDM, the spectral efficiency of the GREENER-OFDM can be expressed as the sum of the spectral efficiencies

of the individual information streams:

$$\eta_{GO}(D) = \sum_{d=1}^D \frac{\eta_U(d)}{2^{d-1}} \quad \text{bits/s/Hz}, \quad (4)$$

where  $\eta_U(d)$  is the spectral efficiency of the U-OFDM stream at depth- $d$ . It is given by [4]:

$$\eta_U(d) = \frac{\log_2(M_d)(N_{\text{FFT}} - 2)}{4(N_{\text{FFT}} + N_{\text{CP}})} \quad \text{bits/s/Hz}, \quad (5)$$

where  $M_d$  is the constellation size at depth- $d$ . In order for the GREENER-OFDM spectral efficiency to match that of DCO-OFDM, the combination of constellation sizes used should satisfy the following constraint:

$$\log_2(M_{\text{DCO}}) = \sum_{d=1}^D \frac{\log_2(M_d)}{2^d}, \quad (6)$$

where  $M_{\text{DCO}}$  is the constellation size of the  $M_{\text{DCO}}$ -QAM DCO-OFDM.

The spectral efficiency ratio of the GREENER-OFDM to the U-OFDM scheme at depth- $d$  can be expressed as the ratio of (4) to (5):

$$\alpha_\eta(D, d) = \frac{\eta_{GO}(D)}{\eta_U(d)} = \frac{\sum_{d=1}^D (\log_2(M_d)/2^d)}{\log_2(M_d)/2}. \quad (7)$$

### C. Power Efficiency

1) *Electrical Power*: The real bipolar OFDM signal can be approximated by a Gaussian distributed random variable with an average power  $E[s^2(t)] = \sigma_s^2$ , where  $\sigma_s$  is the standard deviation of the real bipolar OFDM signal  $s(t)$ , and  $E[\cdot]$  denotes a statistical expectation [4]. Statistics of the U-OFDM signal derived in [9] suggest that the average power of the U-OFDM signal is half that of the bipolar OFDM signal,  $E[s_U^2(t)] = \sigma_s^2/2$ . This is because half of the samples of the U-OFDM signal are equal to zero, while the other half follows a truncated Gaussian distribution. Using the statistics of a truncated Gaussian random variable presented in [12], the mean value of the U-OFDM stream at depth- $d$  can be calculated as  $E[s_d(t)] = \phi(0)\sigma_s/(\gamma_d\sqrt{2^{d-1}})$  where  $1/\gamma_d$  is a scaling parameter for the U-OFDM signal at depth- $d$ ;  $\sigma_s^2$  is twice the power of the unscaled U-OFDM signal at the same depth; and  $\phi(x)$  is the probability density function (pdf) of the standard normal distribution. The average power of the

GREENER-OFDM signal can be expressed as:

$$P_{\text{elec,GO}}^{\text{avg}}(D, \underline{\gamma}) = \mathbb{E}[s_{\text{GO}}^2(t)] = \mathbb{E}\left[\left(\sum_{d=1}^D s_d(t)\right)^2\right]$$

$$= \sigma_s^2 \left( \sum_{d=1}^D \frac{\gamma_d^{-2}}{2^d} + 2\phi^2(0) \sum_{d_1=1}^D \sum_{\substack{d_2=1 \\ d_1 \neq d_2}}^D \frac{(\gamma_{d_1} \gamma_{d_2})^{-1}}{\sqrt{2^{d_1+d_2}}} \right), \quad (8)$$

where  $s_{\text{GO}}(t)$  is the time domain GREENER-OFDM waveform;  $s_d(t)$  is the time domain U-OFDM signal at depth  $d$ ; and  $\underline{\gamma} = \{\gamma_d^{-1}; d = 1, 2, \dots, D\}$  is the set of scaling factors applied to each corresponding stream. The power allocation for each individual stream is optimized with respect to the average power of the modulation signal, which should satisfy the following constraint:

$$P_{\text{elec,GO}}^{\text{avg}}(D, \underline{\gamma}) \leq P_{\text{elec,GO}}^{\text{avg}}(D, \mathbf{1}_{1 \times D}). \quad (9)$$

The electrical SNR of the GREENER-OFDM is defined as [4], [11]:

$$\frac{E_{\text{b,elec}}}{N_o} = \frac{P_{\text{elec,GO}}^{\text{avg}}(D, \underline{\gamma})}{B\eta_{\text{GO}}N_o} = \frac{\mathbb{E}[s_{\text{GO}}^2(t)]}{B\eta_{\text{GO}}N_o}, \quad (10)$$

where  $E_{\text{b,elec}}$  is the electrical energy per bit;  $B$  is the employed bandwidth; and  $N_o$  is the double-sided power spectral density (PSD) of the noise at the receiver.

The increase in average electrical power of the GREENER-OFDM compared with the average electrical power of a scaled U-OFDM at depth- $d$ ,  $P_{\text{elec,U}}^{\text{avg}}(\gamma_d) = \sigma_s^2/(2\gamma_d^2)$ , can be expressed as:

$$\alpha_{\text{elec}}^P(D, \underline{\gamma}) = \frac{P_{\text{elec,GO}}^{\text{avg}}(D, \underline{\gamma})}{P_{\text{elec,U}}^{\text{avg}}(\gamma_d)}. \quad (11)$$

The number of bits conveyed at each depth of a GREENER-OFDM waveform depends on the depth order and the employed constellation size at the respective depth. Therefore, the increase in electrical energy dissipation per bit in the GREENER-OFDM scheme compared to the electrical energy dissipation per bit in an individual U-OFDM stream at depth- $d$  can be obtained from the ratio of (11) and (7), as:

$$\alpha_{\text{elec}}(D, d, \underline{\gamma}) = \frac{\alpha_{\text{elec}}^P(D, \underline{\gamma})}{\alpha_{\eta}(D, d)}. \quad (12)$$

2) *Optical Power*: The average optical power for the GREENER-OFDM can be derived from the expression of the average optical power for the scaled U-OFDM, as:

$$P_{\text{opt,GO}}^{\text{avg}}(D, \underline{\gamma}) = \sum_{d=1}^D \mathbb{E}[s_d(t)] = \phi(0)\sigma_s \sum_{d=1}^D \frac{\gamma_d^{-1}}{\sqrt{2^{d-1}}}, \quad (13)$$

where the optical SNR of the GREENER-OFDM is defined as [4], [11]:

$$\frac{E_{\text{b,opt}}}{N_o} = \frac{P_{\text{opt,GO}}^{\text{avg}}(D, \underline{\gamma})}{B\eta_{\text{GO}}N_o} = \frac{\mathbb{E}[s_{\text{GO}}(t)]}{B\eta_{\text{GO}}N_o}. \quad (14)$$

The optical SNR for a given system configuration can be calculated from the electrical SNR, and vice versa, using the ratio of the electrical average power given in (8) to the optical average power given in (13).

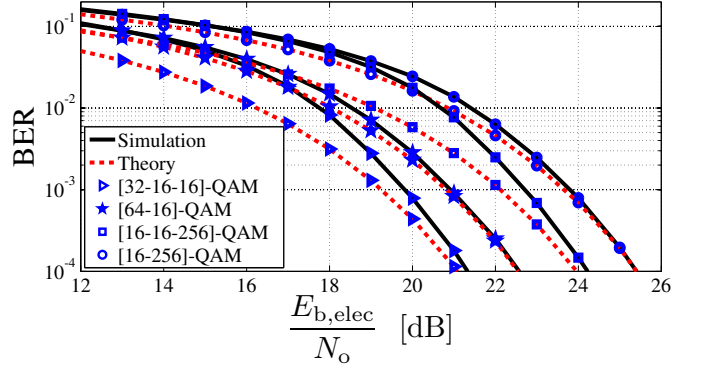


Fig. 2. {[32-16-16], [64-16], [16-16-256], [16-256]}-QAM GREENER-OFDM theoretical and numerical performances comparison as a function of electrical SNR. The scaling factor given in dB for each individual stream at each set is respectively  $\{-1.4, 1.7, 2\}, \{-1.4, 4.8\}, \{4.6, 4.7, -7.2\}, \{7.2, -4.5\}$  as described in (2).

#### IV. THEORETICAL BER ANALYSIS

A theoretical bound on the bit error rate (BER) performance of the different GREENER-OFDM information streams can be derived using the well established formula for the BER performance of real bipolar  $M$ -QAM-OFDM [13], denoted in this paper as  $\text{BER}_{\text{QAM}}$ . A closed-form theoretical bound on the BER performance of the information stream at depth- $d$ , as a function of the electrical SNR, can be estimated by evaluating  $\text{BER}_{\text{QAM}}$  for  $M_d$  and the respective achieved electrical SNR. The achieved electrical SNR at the receiver should be scaled by a factor of 1/2 to account for the SNR loss in U-OFDM, and by a factor of  $1/\alpha_{\text{elec}}(D, d)$  to account for the electrical SNR penalty in the GREENER-OFDM. As a result, the BER performance of the information stream at depth- $d$  as a function of the electrical SNR can be expressed as:

$$\text{BER}_{(D,d,\underline{\gamma})} \cong \text{BER}_{\text{QAM}}\left(M_d, \frac{E_{\text{b,elec}}}{2N_o\alpha_{\text{elec}}(D, d, \underline{\gamma})}\right). \quad (15)$$

The theoretical bound for the BER at depth-1 is expected to match the actual achieved BER at depth-1 because the only source of distortion for that stream is the AWGN at the receiver, since any inter-stream interference caused by the signals at the other depths is completely removed by the subtraction operation during the demodulation process. The BER performance of all streams at higher depths is affected by the BER performance of the streams at the lower depths. Any incorrectly decoded bit at a given depth translates into errors in the iterative stream cancellation process and, in turn, translates into more distortion for all subsequent streams. Deriving the exact BER performance for the information streams at depths higher than depth-1 is an onerous task due to the described error propagation effect. Therefore (15) is presented as a closed-form theoretical lower bound on the achievable BER. The presented solution does not include the effects of the error propagation due to errors in preceding streams which underestimate the BER at low SNR values. For high SNR values, this error propagation effect is assumed to be insignificant due to the low BER expected at each stream,

and the bound is expected to be close to the actual BER performance at each depth.

A closed-form bound on the BER performance of the overall GREENER-OFDM waveform can be obtained by taking a weighted average of the BER bounds at all depths. Since the number of bits conveyed at each depth is different, the BER bound for each stream, given in (15), is weighted by its contribution to the overall spectral efficiency. The overall performance bound can then be expressed as:

$$\text{BER} \cong \frac{1}{D} \sum_{d=1}^D \left( \text{BER}_{(D,d,2)} \frac{\log_2(M_d)/2^d}{\frac{1}{2} \sum_{d=1}^D \log_2(M_d)/2^d} \right). \quad (16)$$

The BER performance bound as a function of the optical SNR can be obtained by inserting the ratio of (13) and (8) into (16).

The validity of the proposed BER performance bound as a function of the electrical SNR and as a function of the optical SNR has been confirmed through Monte Carlo simulations for a large number of possible constellation sizes and power allocations combinations. Fig. 2 compares the theoretical performance bounds with the Monte Carlo simulation results for several combinations of constellation sizes that match the spectral efficiency of 16-QAM DCO-OFDM. The GREENER-OFDM individual streams at each set are scaled by the corresponding optimal scaling factors, which are optimized through extensive search to produce the best performance for the same set of constellation sizes. The theoretical bounds are in close agreement with the Monte Carlo simulation results in all of the presented cases. For  $D = 2$ , the performance bounds coincide almost perfectly with the actual BER values obtained through the numerical simulations. For  $D = 3$ , the bounds are close to the numerical results. However, in all cases they are consistently lower due to the error propagation effect. The examples provided clearly illustrate the effect of error propagation on the performance as the maximum number of information streams in GREENER-OFDM is increased.

## V. SIMULATION RESULTS

The optimal combinations of constellation sizes and their corresponding scaling factors for GREENER-OFDM are obtained using both the theoretical model and Monte Carlo simulations. The optimality is defined as the lowest energy requirements among other spectrally equivalent combinations. The performance of the optimum configurations in GREENER-OFDM is compared with the performance of a spectrally equivalent DCO-OFDM in the context of an ideal front-end linear AWGN channel. The only non-linear effect considered is the negative clipping of the modulation signal due to the characteristics of the ideal LED. Following [12], the DCO-OFDM optimum bias level for the different  $M$ -QAM DCO-OFDM is estimated using Monte Carlo simulations. Results are presented for BER values down to  $10^{-4}$  since most of the forward error correction (FEC) codes would be able to maintain a reliable communication link at such BER values [14]. The optimal scaling factors are given in decibel, as described in (2). The negative values denote that the corresponding streams are amplified, and similarly, the positive values denote that the corresponding streams are attenuated. Fig. 3 presents

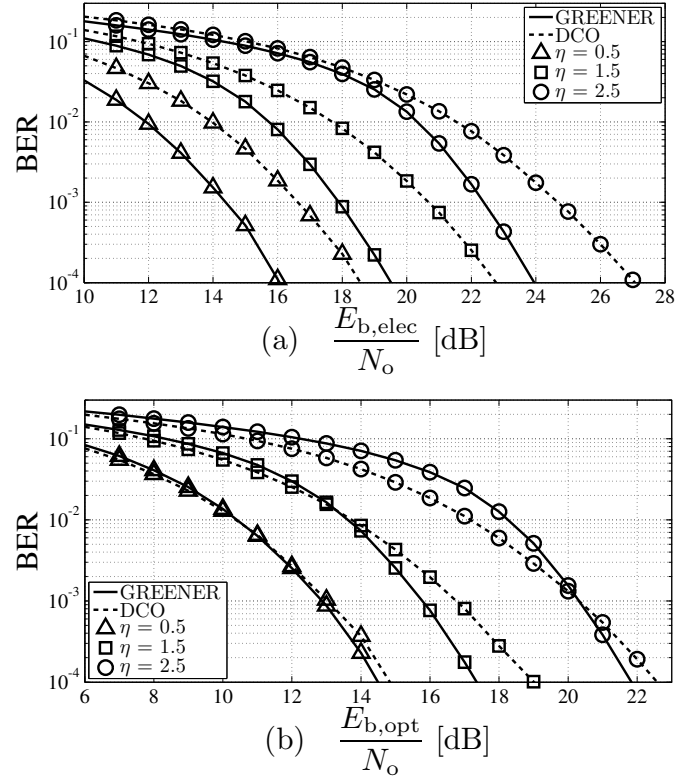


Fig. 3. The performance of GREENER-OFDM vs. the performance of DCO-OFDM for different spectral efficiencies as a function of (a) electrical SNR, and (b) optical SNR. The value of  $\eta$  is given in bits/s/Hz. Optimum biasing levels for DCO-OFDM at  $\eta = \{0.5, 1.5, 2.5\}$  are estimated through Monte Carlo simulations at respectively 6 dB, 7 dB, 8 dB, as described in (1).

a comparison between the performance of GREENER-OFDM and the performance of DCO-OFDM at low spectral efficiencies. At a spectral efficiency of  $\eta = 0.5$  bits/s/Hz, the energy savings of [2-4]-QAM GREENER-OFDM scaled at [2.2,-2.4] dB, respectively, start at 2.6 dB and 0.4 dB for the electrical and optical energy dissipation, respectively, when compared with Binary Phased Shift Keying (BPSK) DCO-OFDM. The energy efficiency of [16-8-4]-QAM GREENER-OFDM scaled at [-1.8,1.4,5] dB, respectively, surpasses that of 8-QAM DCO-OFDM by 3.5 dB for the electrical energy and by 1.5 dB for the optical energy at a spectral efficiency of  $\eta = 1.5$  bits/s/Hz. At a spectral efficiency of  $\eta = 2.5$  bits/s/Hz, [64-64-16]-QAM GREENER-OFDM scaled at [-0.9,-0.7,5.3] dB, respectively, is shown to be more efficient than 32-QAM DCO-OFDM with 3 dB and 0.75 dB electrical and optical energy dissipation, respectively.

Similarly, Fig. 4 presents a comparison between the performance of GREENER-OFDM and the performance of DCO-OFDM for high spectral efficiencies. The results show that [128-128-64]-QAM GREENER-OFDM scaled at [0,-0.4,2.6] dB, respectively, is more efficient than 64-QAM DCO-OFDM with a 3.25 dB lower electrical energy consumption at equivalent optical energy requirements for a spectral efficiency  $\eta = 3$  bits/s/Hz. The electrical energy saving of [512-1024-256]-QAM GREENER-OFDM scaled at [0.5,-2.2,3.8] dB,

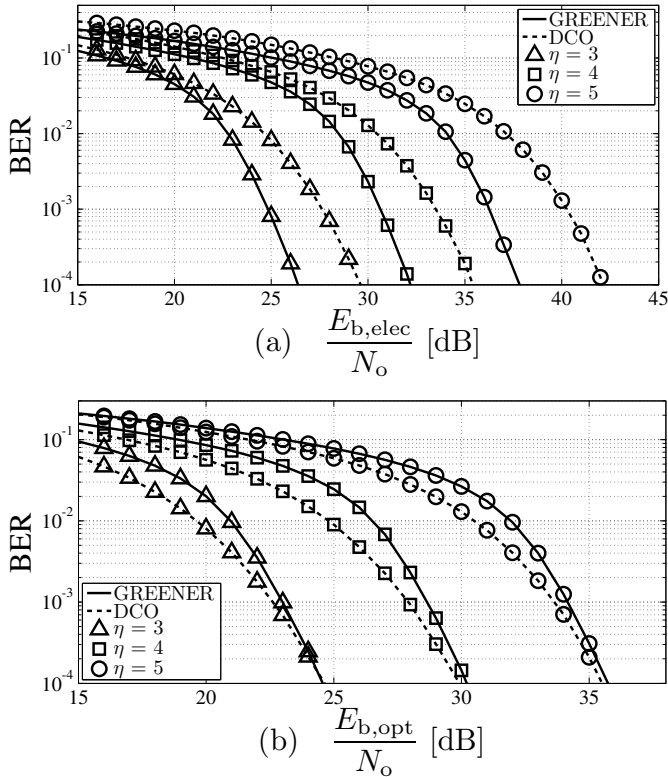


Fig. 4. The performance of GREENER-OFDM vs. the performance of DCO-OFDM for different spectral efficiencies as a function of (a) electrical SNR, and (b) optical SNR. The value of  $\eta$  is given in bits/s/Hz. Optimum biasing levels for DCO-OFDM at  $\eta = \{3, 4, 5\}$  are estimated through Monte Carlo simulations at respectively 9.5 dB, 11 dB, 13 dB, as described in (1).

TABLE I

THE OPTIMAL COMBINATION OF CONSTELLATION SIZES AND SCALING FACTORS FOR DIFFERENT SPECTRAL EFFICIENCIES OF GREENER-OFDM, WHERE  $M_d$  AND  $\gamma_d$  DENOTE THE CONSTELLATION SIZE AND THE SCALING FACTOR FOR THE MODULATION DEPTH- $d$ , RESPECTIVELY. THE SCALING FACTOR  $\gamma_d$  AND THE SPECTRAL EFFICIENCY  $\eta$  ARE PRESENTED IN [dB] AND [bits/sec/Hz], RESPECTIVELY.

DCO-OFDM $M_{DCO-QAM}$	GREENER-OFDM						$\eta$
	$M_1$	$\gamma_1$	$M_2$	$\gamma_2$	$M_3$	$\gamma_3$	
4-QAM	8	-2.3	2	5.9	4	1.4	1
16-QAM	32	-1.4	16	1.7	16	2	2
128-QAM	256	0	256	0	256	0	3.5
512-QAM	2048	-1.9	1024	1.1	256	6.8	4.5

respectively, is 3.36 dB when compared with 256-QAM DCO-OFDM and the optical energy requirements are approximately equivalent in both cases, for a spectral efficiency of  $\eta = 4$  bits/s/Hz. At a spectral efficiency of  $\eta = 5$  bits/s/Hz, [4096-2048-1024]-QAM scaled at [-1.7, 1.4, 4.3] dB, respectively, is more electrically efficient than 1024-QAM DCO-OFDM with savings of 4.3 dB and the optical energy requirements are approximately equivalent in both cases. The optimal combinations of constellation sizes for other spectral efficiency values are given in Table I.

## VI. CONCLUSION

A generalization of the recently introduced concept of enhanced unipolar OFDM is presented. The proposed

GREENER-OFDM allows inherently unipolar OFDM signals to be realized without any spectral efficiency loss when compared with DCO-OFDM. The eU-OFDM is a special case of the GREENER-OFDM with an equivalent modulation order and equal power allocation at each modulation depth. The optimal combinations of constellation sizes and their corresponding scaling factors for GREENER-OFDM have been determined at different spectral efficiencies. A closed-form theoretical bound on the BER performance of the GREENER-OFDM is developed and verified by means of Monte Carlo simulations. The overall performance of the proposed scheme is compared with a spectrally-equivalent DCO-OFDM in the context of a linear LOS AWGN channel. The results suggest that the GREENER-OFDM scheme is superior in performance when compared to DCO-OFDM. In the future, practical implementation studies will consider the nonlinearity effects of the optoelectronic devices that may limit the modulation order.

## ACKNOWLEDGMENT

We acknowledge the support of this research by the Engineering and Physical Sciences Research Council (EPSRC) in the UK under grant EP/K008757/1.

## REFERENCES

- [1] Cisco, "Cisco Visual Networking Index: Global Mobile Data Traffic Forecast Update, 2013-2018," *Cisco White Paper*, 2014.
- [2] D. Tsonev, H. Chun, S. Rajbhandari, J. McKendry, S. Videv, E. Gu, M. Haji, S. Watson, A. Kelly, G. Faulkner, M. Dawson, H. Haas, and D. O'Brien, "A 3-Gb/s Single-LED OFDM-Based Wireless VLC Link Using a Gallium Nitride  $\mu$ LED," *Photonics Technology Letters, IEEE*, vol. 26, no. 7, pp. 637-640, April 2014.
- [3] J. Kahn and J. Barry, "Wireless Infrared Communications," *Proceedings of the IEEE*, vol. 85, no. 2, pp. 265-298, Feb 1997.
- [4] D. Tsonev, S. Sinanovic, and H. Haas, "Complete Modeling of Non-linear Distortion in OFDM-Based Optical Wireless Communication," *Lightwave Technology, Journal of*, vol. 31, no. 18, pp. 3064-3076, Sept 2013.
- [5] J. Carruthers and J. Kahn, "Multiple-Subcarrier Modulation for Nondirected Wireless Infrared Communication," *Selected Areas in Communications, IEEE Journal on*, vol. 14, no. 3, pp. 538-546, Apr 1996.
- [6] J. Armstrong and A. Lowery, "Power Efficient Optical OFDM," *Electronics Letters*, vol. 42, no. 6, pp. 370-372, March 2006.
- [7] S. Lee, S. Randel, F. Breyer, and A. Koonen, "PAM-DMT for Intensity-Modulated and Direct-Detection Optical Communication Systems," *Photonics Technology Letters, IEEE*, vol. 21, no. 23, pp. 1749-1751, Dec 2009.
- [8] N. Fernando, Y. Hong, and E. Viterbo, "Flip-OFDM for Unipolar Communication Systems," *IEEE Transactions on Communications*, vol. 60, no. 12, pp. 3726-3733, Dec. 2012.
- [9] D. Tsonev, S. Sinanović, and H. Haas, "Novel Unipolar Orthogonal Frequency Division Multiplexing (U-OFDM) for Optical Wireless," in *Proc. of the Vehicular Technology Conference (VTC Spring)*. Yokohama, Japan: IEEE, May 6-9 2012, pp. 1-5.
- [10] D. Tsonev and H. Haas, "Avoiding Spectral Efficiency Loss in Unipolar OFDM for Optical Wireless Communication," in *Proc. of the International Conference on Communications (ICC)*. Sydney, Australia: IEEE, Jun., 10-14 2014, pp. 3336-3341.
- [11] J. Armstrong and B. Schmidt, "Comparison of Asymmetrically Clipped Optical OFDM and DC-Biased Optical OFDM in AWGN," *Communications Letters, IEEE*, vol. 12, no. 5, pp. 343-345, May 2008.
- [12] S. Dimitrov, S. Sinanovic, and H. Haas, "Clipping Noise in OFDM-Based Optical Wireless Communication Systems," *Communications, IEEE Transactions on*, vol. 60, no. 4, pp. 1072-1081, April 2012.
- [13] J. Lu, K. Letaief, J.-I. Chuang, and M. Liou, "M-PSK and M-QAM BER Computation Using Signal-Space Concepts," *Communications, IEEE Transactions on*, vol. 47, no. 2, pp. 181-184, Feb 1999.
- [14] ITU-T, "Forward Error Correction for High Bit-Rate DWDM Submarine Systems," in *ITU, Tech. Rep ITU-T G.975.1*. Retrived Jul. 22, 2014 from <http://www.itu.int/rec/T-REC-G.975.1-200402-1/en>, 2003.